Hindawi
Journal of Nanomaterials
Volume 2022, Article ID 2158516, 9 pages
https://doi.org/10.1155/2022/2158516

Research Article

Investigation on Wear Characteristics of AZ91D/ Nanoalumina Composites

M. L. Bharathi,[1] S. Adarsh Rag,[2] L. Chitra,[3] R. Mohammed Ashick,[4] Vikas Tripathi,[5] Srinivasan Suresh Kumar,[6] Sami Al Obaid,[7] Saleh Alfarraj,[8] Mohanraj Murugesan,[9] and Ishwarya Komalnu Raghavan[10]

[1]*Department of Electrical and Electronics Engineering, Sathyabama Institute of Science and Technology, Chennai, Tamil Nadu 600119, India*
[2]*Department of Nanotechnology, Institute of Electronics and Communication Engineering, Saveetha School of Engineering, Saveetha Institutes of Medical and Technical Sciences, Chennai, 602105 Tamil Nadu, India*
[3]*Department of Electrical and Electronics Engineering, Aarupadai Veedu Institute of Technology, Vinayaka Mission's Research Foundation, Paiyanoor, 603104 Tamil Nadu, India*
[4]*Department of Civil Engineering, Sri Sairam Engineering College, Chennai, Tamil Nadu 600044, India*
[5]*Department of Computer Science & Engineering, Graphic Era Deemed to be University, Dehradun, Uttarakhand 248002, India*
[6]*Department of Mechanical Engineering, Panimalar Polytechnic College, Chennai - 600029, Tamil Nadu, India*
[7]*Department of Botany and Microbiology, College of Science, King Saud University, PO Box 2455, Riyadh 11451, Saudi Arabia*
[8]*Zoology Department, College of Science, King Saud University, PO Box 2455, Riyadh 11451, Saudi Arabia*
[9]*Department of Mechanical System Design Engineering, Seoul National University of Science & Technology, Seoul 01811, Republic of Korea*
[10]*Department of ElectroMechanical Engineering, Faculty of Manufacturing, Institute of Technology, Hawassa University, Ethiopia*

Correspondence should be addressed to Ishwarya Komalnu Raghavan; ishwarya138@hu.edu.et

Received 30 November 2021; Accepted 5 January 2022; Published 18 February 2022

Academic Editor: Palanivel Velmurugan

This paper discusses the wear and friction with the 2 W% Al2O3 nanocomposite content of pure Mg and AZ91D Mg alloys. Sliding speeds of 0.5 and 1.5 m/s in cast materials with normal stress conditions have been used in sliding distances up to 2000 m/s (0.5, 1.0, and 1 MPa). In order to evaluate the work hardness of the materials measured on temperature similar to the contact surface, we used hardness patterns and hot-compression flow curves. Mg and AZ91D magnesium alloy pure monolithic Mg are low wear resistant due to an increase in contact temperature due to the adjustment of working conditions, but the wear rate was significantly lower in composite materials, mainly because of nanoparticle strength improvements. Although wear generally contributes to grain refining, increased wear capacity, and greater durability, wear resilience due to dislocation resistance and nanoparticles is seen as the primary wear mechanism in the existing nanocomposites.

1. Introduction

One of the main challenges for energy and greenhouse gas reductions is the development of new structural materials with higher strength/weight ratios in the transport sector. Light metals such as magnesium are therefore very carefully dealt with due to their low-density alloys, high machinability, and availability on the world market. However, magnesium's relative strength, low ambient temperature, ductility, and strength limit the number of applications [1–4]. A traditional way of improving magnesium properties is to combine Al, Zn, Mn, Ca, and others. However, the obtained alloys could not have the mechanical characteristics of compost reinforcement. Moreover, the use of discontinuous micron-to-nanoparticles has been a multitude of studies in the past two decades with several advantages on composites over pure

metals and alloys. One of the best candidates for justifying increasing demand for light weight construction materials in the automotive industry is metal matrix composites (MMCs) [5, 6]. As a matrix for MMCs because of its low density, magnesium is particularly interesting here. However, automotive engines, such as pistons and cylinders, have limited thermal stability and wear resistance. The wear resistance of the Mg matrix is therefore important to hard ceramic particles, particularly on nanoscales, as plastic metal deformation controls wear in accordance with the classic hard Arc model. The enhancement of the metal matrix using hard ceramic nanoparticles can increase strength and hardness, resulting in an increased wear resistance. The most common micron participants were investigating the tribological properties of the composites that have performed a tribological behavior with Mg-Al alloy (A E42) of rare earth with a 20% Saffil fiber [5, 7, 8]. Several papers described both cast and counterfeit alloys material aspects. The AZ31 and ZK60 alloys offer only a good value for money. The process parameters of high-pressure diet magnesium microstructural or mechanical properties were tense bars [9–12]. When pressures were increased and a large overflow cavity blocked, an improved ductility was achieved. There was a good correlation of changes in the microstructure. Magnesium alloys are becoming a promising candidate material for biomedical fixation implant transitory in nature. Magnesium alloys' weak corrosion resistance, on the other hand, severely limits their biological applications. The impact on the interfacial features, microhardness, and the interparticle distance of SiC micropart of the wear Mg and Al MMCs was analyzed. The tribochemical effects of Mg–SiC composites on friction and fretting wear. AZ91 improved wear compliance with SiC microparticles. Different mechanisms were proposed during the study including abrasion, oxidation, delamination and adhesion, and heat softening and melting. Reported nanocomposites with several nanoparticles in the Mg metal matrix had mechanical properties comparable or even better than Mg alloys, or similar composites with significantly greater micron strength. The main mechanical properties emphasized in the research projects studied are traction and stress, hardness, ductility, and toughness of fractures. Despite this, wear and friction studies for Mg nanostrengthening composites are fairly rare. Mg alloys were coated in silica matrix with Al2O3-CeO2 nanocomposites [13–17]. They reported that CeO2 provides better protection against corrosion, and that nano-Al2O3 offers resistance to scratch and wear. Dry, sliding wear of pure magnesium increased in nanosized particles by up to 1.11 volume percent and the continuous load of 10 N over a 1-10 m/s speed range. With increasing volume of reinforcement, nanocomposites show an increased wear resistance. The wear resistance to pure magnesium has increased only 1.11 volume per cent by 1.8 times in the aluminum nanometer particulate matter. Abrasion and adhesion were the principal wear mechanisms for thermal softing with a maximum sliding speed. Nanoparticles' use of Mg matrices from the results of this literary study was not attempted to examine the wear hardening effects of Mg. This report enhances and softens pure Mg and AZ31 friction and wear and wear coefficients with and without Al2O3 nanoparticles while sliding [18–22].

Table 1: Pure magnesium properties.

Properties	Value
Density	1.74 g.cm^{-3}
Melting temperature	645°C
Tensile strength	235 MPa
Modulus of elasticity	46 GPa
Hardness	500 MPa

Figure 1: Pin-on-disc machine.

Table 2: AZ91D magnesium alloy mechanical properties.

Properties	Value
Density	181 g/cm^3
Tensile strength	231 N/mm^2
Yield strength	160 N/mm^2
Percentage of elongation	6%
Hardness value	63 HB

A wide application was discovered in magnesium for magnetic alloys Al and Zn (mostly AZ91 series). The range comprises a range of applications, including steering wheels, dashboards, transmission units, and chassis. For all such applications, corrosion resistance is one requirement. Corrosion patterns of cast magnesium ± aluminum alloys could mainly depend on the structure of phase b and corings and the surrounding environment. The microstructural features vary and produce various corrosion behaviors in the treatment process. Although few studies of AZ91D's impact on corrosion and electrochemical conduct have been previously reported, there still is much ambiguity. Furthermore, during the solidification of the corrosion microstructure, the insufficient distribution of aluminum and zinc is not properly understood. In the majority of those studies, electrochemical evidence supports the interpretation of the impact of multiple microcomponents [23–26]. Moreover, nanomaterials are designed particles with absolutely tiny sizes that take benefit of the nanoscale's distinct physical and chemical capabilities.

Table 3: AZ91D magnesium alloy chemical composition.

Weight %	Mg	Al	Cu	Fe	Zn	Mn	Si	Others
AZ91D Mg alloy	Balance	9.4	0.025	0.004	0.34	0.4	0.1	0.02

There were no attempts to study the working-hardening effects from nanoparticles on wear of the Mg matrices from the results of this literature survey. There are present reports of hardness, modification, and effect on friction and wear coefficients for Mg and AZ91 D pure alloys with and without Al2O3 nanoparticles during sliding wear.

2. Experimental Procedure

2.1. Materials. The atomic no. 12 is magnesium as the symbolic Mg symbol. It is a brilliant grey solid that is physically very similar to the other five elements of the second column (group 2 or earth metals), with the same configuration and crystal structure as each of the elements in group 2.

This element is made from three helium nuclei sequence added into a large old-fashioned star carbon nucleus. When stars such as super ovations explode, a great deal of magnesium is expelled to the interstellar media to restore the new star systems. The eighth most common element in Earth is magnesium. It represents the fourth most common element on earth, 13% of the world's mass, and many of the coat on the planet after iron, oxygen, and silicone: the third most abundant element of seawater after sodium and chlorine [27–29]. Table 1 reveals the pure magnesium properties.

AZ91D is among magnesium alloys with great mechanical properties, corrosion resistance, and portability that is most widely used. Three metal impurities iron, copper, and nickel are applied to the corrosion resistance. It is limited to very low levels, and therefore, primary magnesium is necessary for the production of this alloy. Specific precautions are needed during processing, as with all magnesium alloys. Structural designers should recognize the creep limits of magnesium alloys at higher temperatures while decreasing magnesium alloys' tensile strength, yield, and hardness, while increasing ductility. In addition to environmental effects, a long-term and/or higher temperature change in the structure of metallurgical magnesium also affects mechanical properties. This ageing effect is due to the quick solidification conditions that prevent a striking balance of alloys (effectively, reactions between the alloy constituents have not been completed). As the use of magnesium components at high temperatures is an important consideration, maximum and normal temperature and operating time should be known [4, 6]. Figure 1 reveals the pin-on-disc machine.

Inert, odorless, white amorphous material is commonly called alumina oxide (Al2O3). Table 2 reveals the AZ91D magnesium alloy mechanical properties. Alumina is often used in industrial ceramics. Alumina has contributed to a number of lifelong and society-enhancing applications due to its excellent properties. This medical and modern warfare is widely used. Aluminum oxide is a thermally unstable and nonsoluble compound which occurs naturally as its main ore in different minerals such as corundum, the crystalline

Table 4: Properties of Al_2O_3.

Properties	Value
Density	3.95 g/cm^3
Compressive strength	2500 MPa
Tensile strength	620 MPa
Hardness	15 GPa

version of the oxide, and bauxite [22–24]. Table 3 reveals the AZ91D magnesium alloy chemical composition.

2.2. Processing. Table 4 reveals the properties of Al_2O_3. In order to strengthen pure magnesium and magnesium alloy AZ91D, the matrix and 100 nm Al2 O3 nanoparticles were chosen. At 750,000°C, the Al2O3 master alloy that melts fuel in a protective flow added 2% of its weight to the basic materials (8 wt. percent). The flow of nanoparticles produced a thick adhesive layer to prevent contamination of molten metal [30–32]. The melt was mixed manually and poured into the 250 cc stainless steel mould. Optical microscopy, transmission, and scanning electrons, including grain morphology, strengthening distribution, and worn surfaces, were used to examine the microstructural and macrostructural properties of the material. For 3 samples of optical microscopy, the picric acetic was selected, polished, and etched (1 ml of acetic acid, 1 ml of H2O, 420 mg of picric acid, and 7 ml of ethanol).

2.3. Wear Test. Casting was employed in wear tests for the cross-sectional 24 mm^2 and 11 mm pin specimens. Wear testing with an AISI 52100 stainless steel disc controller was performed using the test material during dry slotting. Each test was performed at a load range of 2.5 and 2.0 m/s at standard loads of 12, 24, and 36 N at pressures of 0.5, 1.0, and 1.5 MPa for sliding games of up to 2000 m. The sliding distance to 0.1 mg determined the weight loss. The discs and the test were cleaned and dried in the air before and after every pollution prevention test with an ultrasound bath of acetone [33–36]. Weight-loss methods were used to inspect wear and removed from worn surfaces, especially when loads of the contact area and the speed sliding are high, before weight loss measures of the highly deformed pin portions squeezed out of the edges.

2.4. Mechanical Testing. The MTS universal test machine's high-tension compressive material tests at an initial strength of 6 to 10/S have been carried out for the purposes of investigating its mechanical temperature at temperatures similar to those of the wear-test interface in deformed materials. The samples were processed and torn into 7 and 10.5 mm diameters. Precompression of the specimens was thermal balance 10 minutes before they were heated at the electric

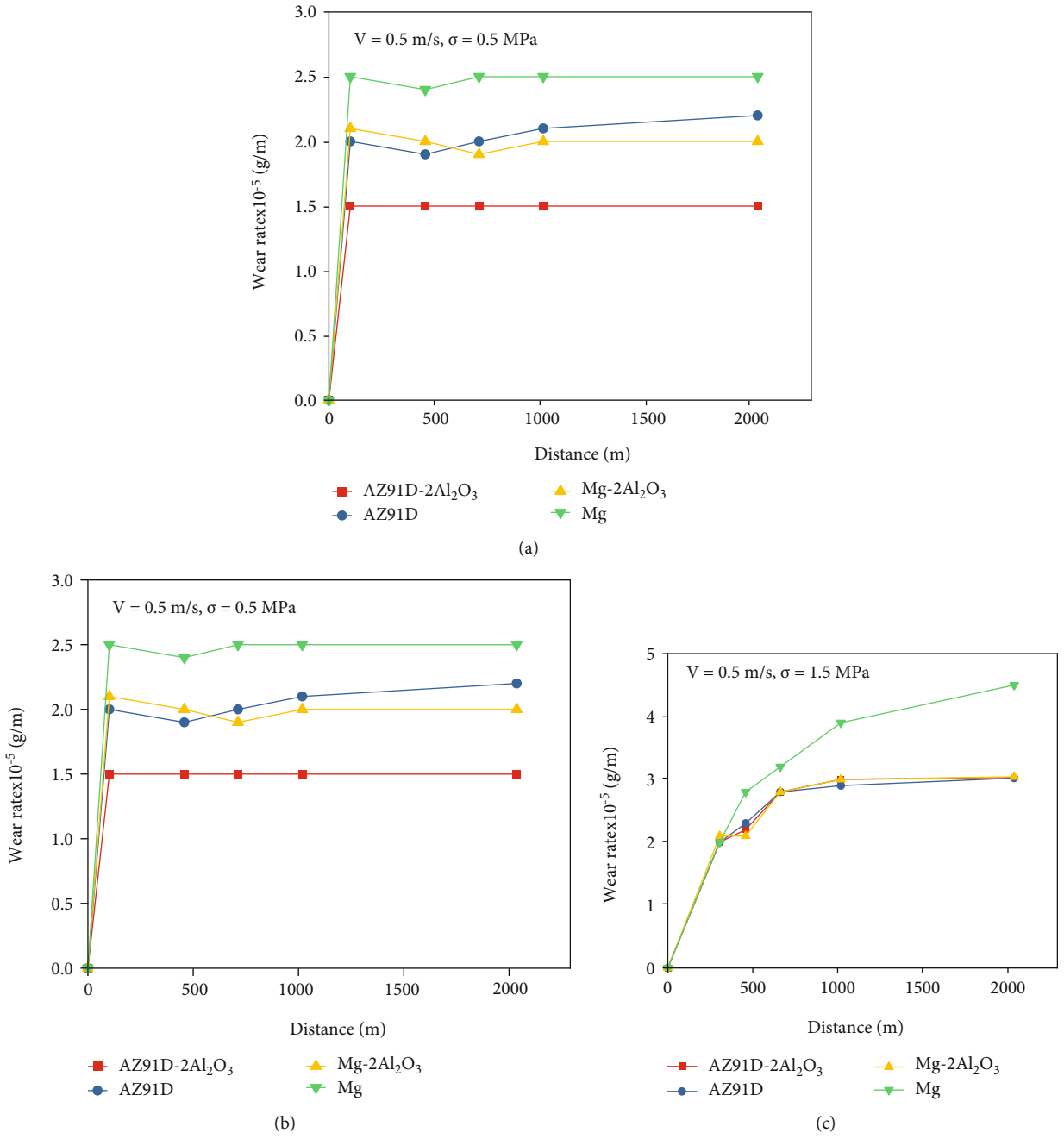

Figure 2: Comparison of materials' wear behavior at sliding speeds $V = 0.5$ m/s and under (a) 0.5, (b) 1.0, and (c) 1.5 MPa contact stresses.

temperature at the desired temperature. PTFE films were used as a lubricant to reduce friction at the test part interface. To determine working hardness, test data have been converted into a true stress strain. These data were then flushed and distinguished by a filter for smoothing. Download 25 gf under Vickers microscope hardness of the samples from the as cast measured for 15 s of dwell time. The cross-section of the samples was polished to demonstrate the hardness profile of the under worn surface. In a test zone with a depth of approximately 200 Nm, microindications were made.

2.5. Constant Immersion Testing. The specimens are continuously polished for constant immersion tests on finer grade emery paper up to 1000 levels. Initially, the G-I-72 standard ASTM procedure cleaned all samples. The polished and prewoven samples are exposed to the solution at different intervals (145 ml, 3.78 percent NaCl). At the end of the experiment, 100 ml of boiling water was cleaned with 15% CrO3 +1% AgCrO4. Acetone washed after that. In millimeters a year, the weight loss was measured, and the rates of corrosion measured in each test. Double experiments have been conducted, and the findings have proved to be expected.

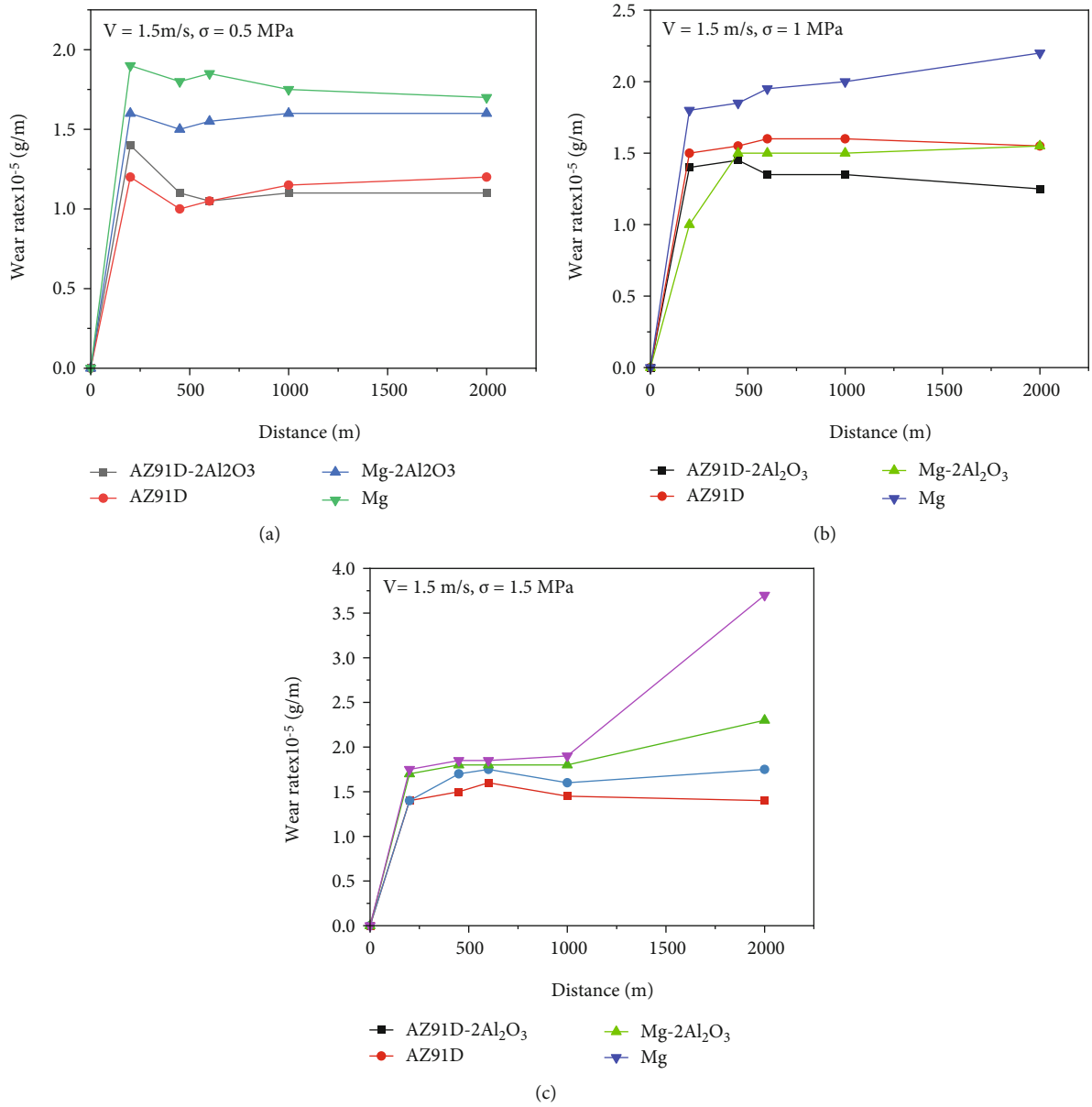

Figure 3: Comparison of material wear behavior with a sliding V velocity of 1.5 m/s and a (a) 0,5 (b) 1.0, and (c) 1.5 MPa contact stress.

2.6. Electrochemical Testing. An automatic laboratory corrosion measurement system has been used for electrochemical polarisation. To this end, electrodes were produced by the connection of a wire with the cold resin on one side of the sample. The solution has been exposed to the opposite specimen surface. The surface was exposed by about 1 cm^2. The specimens were precleaned and washed before each experiment with distilled water and acetone. A standard 3 electrode polarization analysis has been conducted with a 145 ml 3.78% NaCl corrosion cell: a saturated calomel is the platinum electrode reference point, and the electrode tests are performed. The test solution immersed the specimens, resulting in a polarization scan of 1 mVs-1 to nobler values, with the development of a stable status potential.

2.7. In Situ Corrosion Observation. Small droplets of water are usually built on the surface of the material in wet conditions. These droplets contain significant amounts of chloride ions in marine environments. In this minute droplet, several electrochemical cells nucleate and spread. During the present study, a 3.78% NaCl droplet was placed on the material surface, and a ZEISS model of an optical microscope was used to monitor the corrosion phenomena within this minute droplet. The characteristics on the specimen surface have been recorded depending on the time. Scratching technique also examined the passivation behavior.

2.8. Corrosive Media. The whole experiment involved a 3.78% pH NaCl solution with a pH of 7.25. All tests at room temperature were conducted A.R. NaCl used the solution in water distilled.

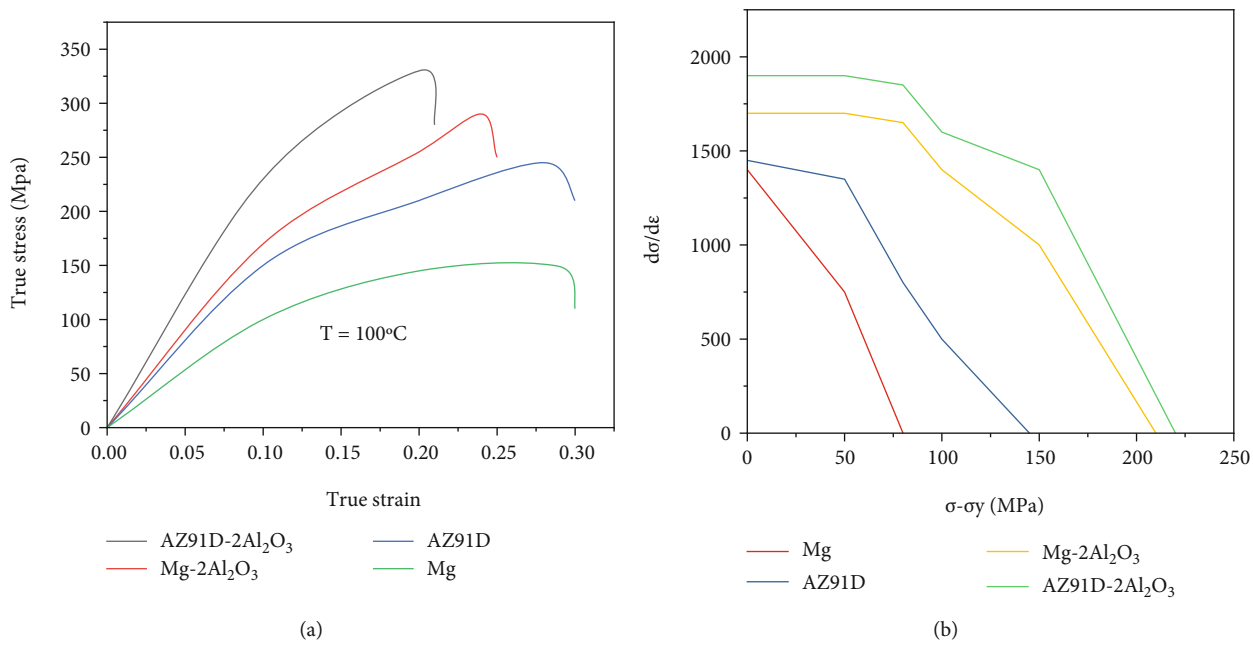

Figure 4: (a) Compression curve high temperature and (b) the appropriate work hardening rates plotted against net flow stress.

3. Result and Discussion

For pure Mg, AZ91D magnesium alloy and nanocomposites wear is measured at various 0.5 and 1.5 m/s stress levels. Under all conditions, nanocomposites have lower wear rates than nonparticles. The material's microstructure reflects the nanoparticles' fineness. The pure Mg is clear, and AZ91D–2Al2O3 is the most sophisticated grain structure. The AZ91 D alloy is available in particular for Mg17Al12 in the finer grain size. Equal distribution of the Mg-2Al2O3 microgram in nanoparticles: the objective is to interact and reinforce the soft matrix of these nanoparticles. The nanoparticles are surrounded by plastic deformation networks. The hardness of wear of materials can be affected by the use due to deformed surface and surface layers.

Compression flow curves at 100°C were obtained and wear rates as demonstrated correlated with work hardening properties of contact surface materials. Flow pressure and UTS are significantly improved in the nanocomposites of pure Mg and AZ91D magnesium alloys. Different work phases have shown that nanostructural testing is superior to monolithic materials, and higher stresses can support the hardness of the work piece. The effect of wear of the higher hardness rates on deformation of the surface layers was shown. The microhardship profiles of the cross-sectional samples used have determined certain conditions. It was found that there are different hardness and softening regimes in free particles and nanocomposite subsurface layers. The specific rates of wear of the test samples are calculated by application and weight loss divided into normal calculation of force and sliding distance. The figure displays better mechanisms of wear and stress, especially at higher glitches. Obviously, nanocomposites' specific wear rates are all less frequently than monolithic materials.

Figure 2 shows the pure Mg, AZ91D, and nanocomposites wear rates at constant 0.5 m/s for different stresses. It is evident that Mg and AZ91D contain less wear than particle-free specimens under all conditions. The same behavior with 1.5 m/s sliding speed and 0.5, 1, and 1.5 MPa stress is seen with Figure 3. As the Archard's equation suggests, higher nanosubstances are directly linked to greater hardness and strength. The use of hard ceramic nanoparticles in the soft matrix by a combination of various parameters allows improvements in hardness and strength. These nanoparticles play the main role in the solidification of MMCs as nuclear sites.

Figures 2 and 3 show a constant sliding distance wear rate of 0.5 and 1 MPa for all materials that have been tested at normal stresses, but only nanocomposites can demonstrate this at a higher slid rate of 1.5 mm/min under the standard 2 MPa stress (Figure 3(c)). During sliding, surface dislocation interactions can produce a high density of dislocation networks, allowing dislocation of particle free matrices to be further enhanced. Increased normal stresses could overcome the back stress of dislocation networks, which can lead to the softening of the matrix by tangential stresses. This can improve the wear rate at higher rankings. However, in all circumstances, nanocomposite wear rates (i.e., Mg-2Al2O3 and AZ91D-2AL2O3), particularly with all experiment and sliding speeds other than the ones in Figure 1(c), remained constant during sliding distance. In addition to the enhanced interaction of disruptions, Mg17 Al12 may also contribute to trap dislocation and thus increase the capacity of the matrix work in AZ91D and non-sharable nanotechnology in composite samples. Figures 2 and 3 are comparison showing lower rates of sample wear at 1.5 m/s sliding speeds with the same normal stress. At 1.5 m/s sliding speed AZ91D-2Al2O3, wear rate decreased

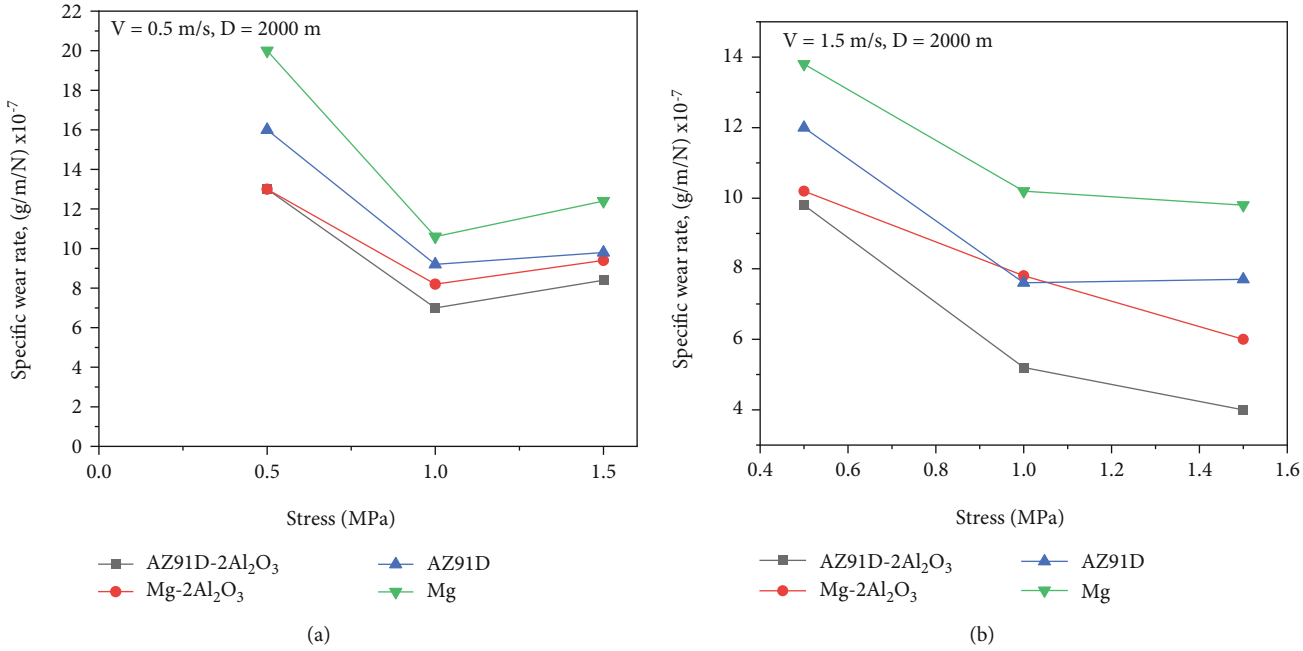

Figure 5: Test materials have a specific wear rate of (a) 0.5 and (b) 1.5 m/s at sliding speeds.

by roughly 25% compared to 0.5 m/s, for example, with regular stress 0.5 MPa. Increased surface and subsurface stress hardness and stress hardening can be attributed to increased stress at higher rates.

The rate of wear is higher than in Figure 3(c), and the rate of wear is 1.5 m/s at sliding speed and 0.5 m/s at sliding rhythm. This behavior could be explained by more relaxation than hard work in Figure 2(c) at lower sliding speeds of 0.5 m/s. While a high sliding speed of 1.5 m/s is expected to produce a strong heat release due to high thermal friction, the effects of dissipation appear to have been controlled by a higher-pressure resistance rate. In Figure 3(c) after 1000 m sliding, the wear rate for Mg and a lower AZ91D level is also evident. The reduced hardness of monolithic samples can be attributed to this. This is consistent with the lower nanocomposite wear rate, which sometimes compensates for the observed weakness through greater resilience. Mg17Al12 reduces nanocomposite AZ91D base presence and hardening. Figure 3(c) shows that after 1000 m of sliding distance, AZ91D is adjusted to 1.5 m/s lower than 1.5 MPa. However, thermal adjustment in samples of Mg started under the lower normal stress of 1 MPa, as shown in Figure 3(b). For nanoparticles with sliding distance inhibition works, more consistent wear rates were demonstrated in Figure 3(c). In other words, the thermal interface softening effect is dominated by nanoparticle hardening.

Phase 3 sample hardening trends in phases II and III are very much in line with the work hardening in Kocks-Mecking (KM). Due to the lower dislocation density, dislocations can increase during phase II hardening during deformation. Figure 4(a) reveals compression curves at high temperature. According to Figure 4(b), it was possible to achieve a dynamic recuperation of stage 3 after the hardening stage when forests and loops are relaxed as cells and walls of dislocation. Figures 5(a) and 5(b) show that test materials have a specific wear rate of 0.5 and 1.5 m/s at sliding speeds.

4. Conclusion

Wear resistance is improved by including a two wt—% Al2O3 pure Mg and AZ91D Mg alloy. Hard work and relaxation of nanocomposites and composite enhancement mechanisms were discovered as fundamental factors in charging hard particles and inadequate hardening. The wear and tear of high-speed nanomaterials and everyday sliding stress are controlled by the coincidence of high sliding rates and loads between thermal softening and hard work due to deformation and strengthening of particles. A more extensive phase II and a smaller hard work space in stage III demonstrated the increased expectation of working life in nanocomposites. In addition to improved mass hardness, this provides a matrix for adherence to oxides and lowers nanocomposite friction coefficients. The absence of high-speed thermal suppression and natural stresses in nanocompounds is related to the formation of oxide coatings and the accumulation of stress. Various systems were detected during dry wear during abrasion, oxidation, and delamination and pure Mg, AZ91D, and its nanocomposites.

Data Availability

The data used to support the findings of this study are included within the article. Further data or information is available from the corresponding author upon request.

Conflicts of Interest

The authors declare that there are no conflicts of interest regarding the publication of this paper.

Acknowledgments

The authors thank Sri Sairam Engineering College, Chennai, and Sathyabama Institute of Science and Technology, Chennai, for providing technical assistance to complete this experimental work. This project was supported by Researchers Supporting Project number (RSP-2021/315) King Saud University, Riyadh, Saudi Arabia.

References

[1] O. Fruhwirth, G. W. Herzog, I. Hollerer, and A. Rachetti, "Dissolution and hydration kinetics of MgO," *Surface Technology*, vol. 24, no. 3, pp. 301–317, 1985.

[2] T. Sathish, V. Mohanavel, K. Ansari et al., "Synthesis and characterization of mechanical properties and wire cut EDM process parameters analysis in AZ61 magnesium alloy+ B4C + SiC," *Materials*, vol. 14, no. 13, p. 3689, 2021.

[3] A. Chandrashekar, V. Mohanavel, A. R. Kaladgi et al., "The investigation of the effect of nano particles on dry sliding wear and corrosion behavior of Al-Mg/Al2O3 composites," *surface topography: metrology and properties*, vol. 9, no. 4, 2021.

[4] R. Ambat, N. N. Aung, and W. Zhou, "Studies on the influence of chloride ion and pH on the corrosion and electrochemical behaviour of AZ91D magnesium alloy," *Journal of Applied Electrochemistry*, vol. 30, no. 7, pp. 865–874, 2000.

[5] D. Daloz, P. Steinmetz, and G. Michot, "Corrosion behavior of rapidly solidified magnesium-aluminum-zinc alloys," *Corrosion*, vol. 53, no. 12, pp. 944–954, 1997.

[6] R. Ambat, N. N. Aung, and W. Zhou, "Evaluation of microstructural effects on corrosion behaviour of AZ91D magnesium alloy," *Corrosion Science*, vol. 42, no. 8, pp. 1433–1455, 2000.

[7] T. J. Warner, N. A. Thorne, G. Nussbaum, and W. M. Stobbs, "A cross-sectional TEM study of corrosion initiation in rapidly solidified Mg-based ribbons," *Surface and Interface Analysis*, vol. 19, no. 1-12, pp. 386–392, 1992.

[8] J.-F. Nie, I. J. Polmear, and D. S. S. John, *Light Alloys: Metallurgy of the Light Metals*, Elsevier, 2017.

[9] W. A. Badawy, M. M. El-Rabiee, N. H. Helal, and H. Nady, "Effect of nickel content on the electrochemical behavior of Cu–Al–Ni alloys in chloride free neutral solutions," *Electrochimica Acta*, vol. 56, no. 2, pp. 913–918, 2010.

[10] O. Khaselev and J. Yahalom, "The anodic behavior of binary Mg-Al alloys in KOH-aluminate solutions," *Corrosion Science*, vol. 40, no. 7, pp. 1149–1160, 1998.

[11] O. Lunder, J. E. Lein, T. K. Aune, and K. Nisancioglu, "The role of Mg17Al12 phase in the corrosion of Mg alloy AZ91," *Corrosion*, vol. 45, no. 9, pp. 741–748, 1989.

[12] G. Song, A. Atrens, and M. Dargusch, "Influence of microstructure on the corrosion of diecast AZ91D," *Corrosion Science*, vol. 41, no. 2, pp. 249–273, 1998.

[13] I. J. Polmear, "Magnesium alloys and applications," *Materials Science and Technology*, vol. 10, no. 1, pp. 1–16, 1994.

[14] K. U. Kainer and B. L. Mordike, *Magnesium Alloys and their Applications*, Wiley-VCH Weinheim, 2000.

[15] S. Vasisht, A. Tsvetkov, and T. Troczynski, "Ceramic Master Alloy for Grain Refinement and Modification of Aluminum Alloys," in *AUTO21 Conference*, Barrie, Ontario, Canada, 2006.

[16] N. Afrin, D. L. Chen, X. Cao, and M. Jahazi, "Strain hardening behavior of a friction stir welded magnesium alloy," *Scripta Materialia*, vol. 57, no. 11, pp. 1004–1007, 2007.

[17] U. F. Kocks and H. Mecking, "Physics and phenomenology of strain hardening: the FCC case," *Progress in Materials Science*, vol. 48, no. 3, pp. 171–273, 2003.

[18] H. Mecking and U. F. Kocks, "Kinetics of flow and strain-hardening," *Acta Metallurgica*, vol. 29, no. 11, pp. 1865–1875, 1981.

[19] Z. Zhang and D. L. Chen, "Contribution of Orowan strengthening effect in particulate-reinforced metal matrix nanocomposites," *Materials Science and Engineering A*, vol. 483, pp. 148–152, 2008.

[20] C. S. Goh, J. Wei, L. C. Lee, and M. Gupta, "Properties and deformation behaviour of mg–Y2O3 nanocomposites," *Acta Materialia*, vol. 55, no. 15, pp. 5115–5121, 2007.

[21] X. Wang, J. D. Embury, W. J. Poole, S. Esmaeili, and D. J. Lloyd, "Precipitation strengthening of the aluminum alloy AA6111," *Metallurgical and Materials Transactions A: Physical Metallurgy and Materials Science*, vol. 34, no. 12, pp. 2913–2924, 2003.

[22] L. M. Cheng, W. J. Poole, J. D. Embury, and D. J. Lloyd, "The influence of precipitation on the work-hardening behavior of the aluminum alloys AA6111 and AA7030," *Metallurgical and Materials Transactions A: Physical Metallurgy and Materials Science*, vol. 34, no. 11, pp. 2473–2481, 2003.

[23] A. R. Phani, F. J. Gammel, and T. Hack, *Retracted: structural, mechanical and corrosion resistance properties of Al2O3–CeO2 nanocomposites in silica matrix on Mg alloys by a sol–gel dip coating technique*, Elsevier, 2006.

[24] W. L. E. Wong and M. Gupta, "Improving overall mechanical performance of magnesium using nano-alumina reinforcement and energy efficient microwave assisted processing route," *Advanced Engineering Materials*, vol. 9, no. 10, pp. 902–909, 2007.

[25] K. S. Tun and M. Gupta, "Improving mechanical properties of magnesium using nano-yttria reinforcement and microwave assisted powder metallurgy method," *Composites Science and Technology*, vol. 67, no. 13, pp. 2657–2664, 2007.

[26] L. Lu, K. K. Thong, and M. Gupta, "Mg-based composite reinforced by Mg2Si," *Composites Science and Technology*, vol. 63, no. 5, pp. 627–632, 2003.

[27] C. Y. H. Lim, D. K. Leo, J. J. S. Ang, and M. Gupta, "Wear of magnesium composites reinforced with nano-sized alumina particulates," *Wear*, vol. 259, no. 1–6, pp. 620–625, 2005.

[28] C. Y. H. Lim, S. C. Lim, and M. Gupta, "Wear behaviour of SiCp-reinforced magnesium matrix composites," *Wear*, vol. 255, no. 1–6, pp. 629–637, 2003.

[29] B. V. M. Kumar, B. Basu, V. S. R. Murthy, and M. Gupta, "The role of tribochemistry on fretting wear of Mg-SiC particulate composites," vol. 36, no. 1, pp. 13–23, 2005.

[30] S. K. Thakur and B. K. Dhindaw, "The influence of interfacial characteristics between SiCp and Mg/Al metal matrix on wear, coefficient of friction and microhardness," *Wear*, vol. 247, no. 2, pp. 191–201, 2001.

[31] A. K. Mondal, B. S. S. C. Rao, and S. Kumar, "Wear behaviour of AE42+20% saffil mg-MMC," *Tribology International*, vol. 40, no. 2, pp. 290–296, 2007.

[32] J. Archard, "Contact and rubbing of flat surfaces," *Journal of Applied Physics*, vol. 24, no. 8, pp. 981–988, 1953.

[33] B. L. Mordike and T. Ebert, "Magnesium: properties—applications—potential," *Materials Science and Engineering A*, vol. 302, no. 1, pp. 37–45, 2001.

[34] H. Z. Ye and X. Y. Liu, "Review of recent studies in magnesium matrix composites," *Journal of Materials Science*, vol. 39, no. 20, pp. 6153–6171, 2004.

[35] A. A. Voevodin and J. S. Zabinski, "Nanocomposite and nanostructured tribological materials for space applications," *Composites Science and Technology*, vol. 65, no. 5, pp. 741–748, 2005.

[36] S. F. Hassan and M. Gupta, "Enhancing physical and mechanical properties of Mg using nanosized Al2O3 particulates as reinforcement," *Metallurgical and Materials Transactions A: Physical Metallurgy and Materials Science*, vol. 36, no. 8, pp. 2253–2258, 2005.